

Research Article

MOLECULAR PAIN

Exacerbation of paclitaxel-induced neuropathic pain behaviors in breast tumor-bearing mice

Molecular Pain Volume 21: 1–11 © The Author(s) 2025 Article reuse guidelines: sagepub.com/journals-permissions DOI: 10.1177/17448069251380034 journals.sagepub.com/home/mpx



Hee Kee Kim^{1*}, Juping Xing^{2*}, Youn-Sang Jung³, Jae-II Park⁴, Hee Young Kim², Jimin Kim⁵, and Salahadin Abdi⁶

Abstract

Background: Chronic pain and cancer interact bidirectionally, with pain enhancing sensory peptides and potentially promoting tumor growth. Despite this, most chemotherapy-induced neuropathic pain (CIPN) studies overlook the contribution of cancer itself to neuropathy, focusing instead on chemotherapy-induced mechanisms. Animal models of chemotherapy-induced neuropathic pain (CINP) have been developed by injecting chemotherapeutic drugs such as paclitaxel into normal animals without cancer. This study aimed to develop a new model in mouse mammary tumor virus—polyomavirus middle T antigen (MMTV-PyMT) mice, a widely used breast cancer model with normal immune function.

Results: The percentage of positive response (PPR) of paclitaxel-injected MMTV-PyMT mice increased (about 20%; baseline, 10%) on day 4, reached the highest levels (50%–60%) on days 6–9, and then plateaued by day 29. In comparison, the PPR of paclitaxel-injected C57BL/6 was less than 10% on days 0–6, was about 40% on day 9, and then plateaued by day 29. Breast tumor—bearing mice exhibited an earlier onset and greater severity of paclitaxel-induced pain behaviors than tumor-free C57BL/6 mice. Systemic LGK-974 ameliorated paclitaxel-induced pain behaviors in MMTV-PyMT mice. Active β-catenin was detected in neurons and satellite cells of the dorsal root ganglia. Conclusions: Paclitaxel-induced neuropathic pain model in breast tumor—bearing female MMTV-PyMT mice may be a useful animal model for investigating the analgesic effects and underlying mechanisms for CINP in breast cancer patients as well as the interplay between CINP development and cancer progression.

Keywords

Paclitaxel, neuropathic pain, breast tumor

Date Received: 19 August 2025; Revised 26 August 2025; accepted: 2 September 2025

*These authors contributed equally to this work and share first

Corresponding Authors:

Hee Young Kim, Department of Physiology, Yonsei University College of Medicine, Yonsei Ro 50-1, seoul, South 03722, South Korea. Email: heeykim@yuhs.ac

Hee Kee Kim, Southern Reformed College & Seminary, Houston, TX 77084, USA.

Email: kimheekee@gmail.com



¹Southern Reformed College & Seminary, Houston, TX, USA

²Department of Physiology, Yonsei University College of Medicine, Seoul, Republic of Korea

³The Department of Life Science, Chung-Ang University, Seoul, Republic of Korea

⁴The Department of Experimental Radiation Oncology, Division of Radiation Oncology; Graduate School of Biomedical Sciences; Program in Genetics and Epigenetics, The University of Texas MD Anderson Cancer Center, Houston, TX, USA

⁵University of the Incarnate Word School of Osteopathic Medicine, San Antonio, TX, USA

⁶Division of Anesthesiology, Critical Care & Pain Medicine, The Department of Pain Medicine, The University of Texas MD Anderson Cancer Center, Houston, TX, USA

Introduction

Patients with cancer often develop hard-to-treat peripheral neuropathic pain due to tumors themselves, which can press on nerves, as well as cancer treatments including surgery, radiation, and chemotherapy.1 In addition, many chemotherapeutic drugs including taxanes (i.e. paclitaxel and docetaxel), platinum-based compounds (i.e. cisplatin and oxaliplatin), vinca alkaloids (i.e. vincristine and vinblastine), and proteasome inhibitors (i.e. bortezomib) can produce neuropathic pain, termed chemotherapy-induced neuropathic pain (CINP).² The symptoms of CINP include allodynia, hyperalgesia, tingling, numbness, and ongoing burning pain in a "stocking and glove" distribution.³ In particular, paclitaxel is associated with a particularly high incidence of chemotherapy-induced peripheral neuropathy (CIPN) in patients because it is widely used to treat breast cancer, cervical cancer, ovarian cancer, and non-small cell lung carcinomas. 4 Neurological adverse effects by chemotherapeutic drugs include abnormal function of primary sensory nerves, activation of ion channels, abnormal windup of the spinal dorsal horn, activation of immune cells, and induction of inflammatory cytokines.³ While chemotherapeutic agents are administered in cancer patients in clinic, almost all animal CIPN models have been made by using cancer-free normal animals.⁵ Several studies have proven bidirectional interactions between sensory neurons and cancer.6 Chronic pain increases the expression of sensory-located peptides and growth factors and can promotes cancer growth. Enhanced expression of pain-related peptides is found in sensory neurons in cancer-bearing mice.8 While almost all CIPN studies have focused on the pain due to chemotherapy-related neurotoxicity, the role of cancer in the development of CIPN has been largely ignored.

Breast cancer is one of the most common cancers in women worldwide and makes a significant impact on the health of women. Various breast cancer animal models such as spontaneous, induced, transplanted, and transgenic models have been employed to study breast cancer. 10 In particular, the mouse mammary tumor virus-polyomavirus middle T antigen (MMTV-PyMT) model is widely used as a transgenic breast cancer animal model because of its rapid breast tumor development (within 4-8 weeks after birth) and high lung metastasis rate within 14 weeks (85% of mice). 11 The MMTV-PyMT model uses MMTV long terminal repeat promoter to drive the expression of PyMT, an overexpressing breast cancer-specific oncogene.¹² Further, many reports show that the MMTV-PyMT model is pathologically relevant to human breast cancer. Furthermore, Wnt/β-catenin signaling plays a major role in cell proliferation and differentiation and has been tightly associated with varous cancers including breast cancer. 13,14 It was also reported that Wnt/βcatenin signaling is involved in the development of an expression of neuropathic pain.¹⁵ Nevertheless, the role of Wnt/β-catenin signaling in CIPN under cancer conditions remains unclear.

Therefore, the aims of this study were to compare the development of neuropathic pain between normal and breast tumor–bearing mice and investigate the mediation of Wnt/ β -catenin signaling in development of neuropathic pain in tumor-bearing mice.

Methods

Searching in vivo breast cancer animal models for the selection of breast tumor—bearing MMTV-PyMT mice

To select a breast tumor animal model for neuropathic pain, the characteristics of various breast tumor animal models were searched based on whether animal models had 1) spontaneous tumor formation, 2) normal immune function, and 3) normal behavioral activity.

Experimental animals

Adult female C57BL/6 mice (15–25 g; Charles River) and adult female MMTV-PyMT transgenic mice (15–30 g; Jackson Laboratory) were used. Mice had free access to food and water under a normal light/dark cycle (light cycle: 7AM to 7PM) in transparent plastic cages. The experimental protocol was approved by the Institutional Animal Care and Use Committee at The University of Texas MD Anderson Cancer Center (Houston, TX, USA).

Paclitaxel-induced neuropathic pain (PINP) model in C57BL/6 mice and breast tumor—bearing MMTV-PyMT Mice

PINP was induced as previously described.^{16–18} Paclitaxel (GenDepot) was dissolved in dimethyl sulfoxide (DMSO) at a concentration of 50 mg/ml and stored in a freezer (–80 °C). Before injection, the stock solution was mixed with an equal volume of Tween 80 and then diluted with sterile saline to a concentration of 0.4 mg/ml. In the MMTV-PyMT group, mammary tumors were observed by palpation twice or three times per week. When the tumor diameter reached 0.5 cm, we began paclitaxel or vehicle injections (day 0).

To induce PINP in normal C57BL/6 mice or MMTV-PyMT mice, paclitaxel (4 mg/kg, 0.8% DMSO and 0.8% Tween 80 in sterile saline, 10 ml/kg) was injected intraperitoneally on days 0, 2, 4, and 6.16 After injection, mechanical hypersensitivity and body weight were monitored. When the tumor diameter in MMTV-PyMT mice approached 2 cm, the animals were euthanized, and their tumors resected and photographed.

Measurement of mechanical hypersensitivity

Mechanical hypersensitivity was determined by measuring the PPR to stimulus under blinded conditions.¹⁶ For each test, the mouse was placed in a plastic chamber on the top of

a mesh screen platform and was habituated for 15 min. The 0.1-g von Frey filament was applied to the most sensitive areas (the base of the third and fourth digits and the base of the fourth and fifth digits) of the left hind paw with sufficient force to bend the filament slightly for 2–3 s. This stimulus was applied 10 times to each mouse at 2-minute intervals. Positive responses were defined by the abrupt withdrawal or licking of the foot during stimulation or immediately after stimulus removal. The PPR was then calculated as the percentage of the number of positive responses per 10 stimuli.

Behavioral testing for sedation

To determine whether paclitaxel or LGK-974 induced sedation in mice, we measured the mice's sedation status using 5-point (0–4) scales of posture (0 = normal, 4 = flaccid atonia) and righting reflexes (0 = struggles, 4 = no movement) as previously described.¹⁸ Sedation tests were performed immediately after each mechanical hypersensitivity test because sedation could produce less responses of mechanical hypersensitivity.

Intraperitoneal injection of LGK-974

LGK-974 (MedChemExpress) was dissolved in DMSO, suspended in 1% sodium carboxymethyl cellulose in phosphate-buffered saline without calcium and magnesium, and administered to the paclitaxel-treated MMTV-PyMT mice via intraperitoneal injection. ¹⁶ To determine the single-dose and multiple-dose analgesic effects of LGK-974, we administered a single intraperitoneal injection (1, 3, or 10 mg/kg, n=6) on day 14 and multiple intraperitoneal injections of 10 mg/kg twice daily on days 14-18 (n=6). Vehicle-injected mice received an equivalent volume (10 ml/kg) of 1% sodium carboxymethyl cellulose in phosphate-buffered saline without LGK-974 (n=6).

Immunohistochemical analyses of DRG

The L4 and L5 DRGs were collected from vehicle-injected C57BL/6 mice (n = 3), vehicle-injected MMTV-PyMT mice (n = 3), and paclitaxel-injected MMTV-PyMT mice (n = 3)on days 14–20 after the first paclitaxel or vehicle injection. The L4 and L5 DRGs were fixed, cryosectioned, and mounted on microscope slides. 16 The sections were incubated with combinations of the primary antibodies to nonphospho active β-catenin (a marker for canonical Wnt signaling pathway; rabbit, 1:100, Cell Signaling Technology), NeuN (neuron marker, mouse, 1:50, Abcam), calcitonin gene-related peptide (CGRP; peptidergic somatosensory neuronal marker; mouse, 1:50, Santa Cruz Biotechnology), or glial fibrillary acidic protein (GFAP; satellite cell marker; mouse, 1:100, Santa Cruz Biotechnology) overnight at 4 °C and then incubated with secondary antibodies with Alexa Fluor 568 or Alexa Fluor 488 (goat anti-rabbit with Alexa

Fluor 488, 1:100, GenDepot; or goat anti-mouse with Alexa Fluor 594, 1:100, GenDepot). In addition, ProLong Diamond Antifade Mountant was applied to the sections. The stained tissue sections were viewed under a Vectra 2 microscope from PerkinElmer.

Statistical analyses

Data were summarized as means with standard errors of the mean for behavioral testing and body weight. The data were analyzed using GraphPad Prism 6 software and two-way repeated-measures analyses of variance with one repeated factor (time), followed by the Tukey *post hoc* test for behavioral testing and body weight. In all cases, P < 0.05 was considered statistically significant.

Ethics Statement

All animal procedures were approved by the Institutional Animal Care and Use Committee (IACUC) at The University of Texas MD Anderson Cancer Center (Approval Nos. 00001569-RN00 and 11-12-12541), and were conducted in full accordance with the relevant guidelines and regulations, including the ARRIVE guidelines and the U.S. National Research Council's Guide for the Care and Use of Laboratory Animals. All efforts were made to minimize animal suffering and reduce the number of animals used.

Mice were housed under a 12-hour light/dark cycle with free access to food and water. All behavioral assessments and treatments were performed under blinded conditions. Anesthesia was administered with isoflurane (2%–3% in oxygen) before all invasive procedures. At the study endpoint or when tumors reached 2 cm in diameter, mice were euthanized by carbon dioxide (CO₂) inhalation followed by cervical dislocation, in compliance with institutional and federal guidelines.

Results

Summary of in vivo breast cancer animal models for the selection of MMTV-PyMT mice

We searched the literature for all types of breast cancer animal models, i.e. 1) spontaneous, 2) induced, 3) transplanted, and 4) genetically engineered models and summarized our findings in Table 1.^{10,12,19,20} Ultimately, we selected the MMTV-PyMT mice model for this study because this model has normal animal behavior, normal immune function, spontaneous breast tumor formation, and commercial availability.

Sedation

Because sedation can produce a false analgesic effect, we measured sedation based on posture and righting reflexes of all C57BL/6 and MMTV-PyMT mice injected with

| | u | • |
|---|---|---|
| • | d | |
| • | ζ | |
| | ۲ | |
| | 2 | |
| | Š | |
| ٠ | È | |
| | č | |
| | 9 | |
| | ۲ | |
| | 5 | |
| | ÷ | |
| | č | |
| | 2 | |
| (| Ÿ | |
| | | • |
| • | - | |
| | 0 | ľ |
| 1 | c | |
| • | C | |
| ı | | |

| Table 1. Breast cancer animal models | t cancer animal | models | | | |
|---------------------------------------|------------------------|--|--|---|---|
| Model | | Methods | Examples | Disadvantages | Advantages |
| Spontaneous | | No treatment | C3H, A, CBA/J, TA2 mice | Low incidence rates and long latency | Naturally occuring spontaneous tumors occur in genetically heterogeneous |
| Induced | Chemical | DMBA and NMU | DMBA-induced SD rats, NMU-induced SD, BUF/N, and F344 rats | Low efficiencies, long incubation times, different incidence times, anddifferent pathological characteristics | High incidence rates; short latencies; and more reliable, predicted results |
| | Physical Biological | Radiation Lentivirus infection | Radiation-induced SD and Lewis rats | Radiation use Virus use | |
| Transplanted | Allograft | Spontaneous or induced breast cancer cells transplanted into the same strain | Tansplant breast cancer cell in immunodeficient mice | Immunodeficient mice (nude mice, NOD-SCID mice, and NSG mice) | Short cycles, small variations, and high tumor formation rates |
| | Xenograft | Human breast cancer cells or patient tumor tissues | Transplant cell-derived xenografts or patient tumor in immunodeficient mice | Immunodeficient mice | Short cycles, small variations, and high tumor formation rates |
| Genetic engineering mouse model | Transgenic | Oncogene activation | MMTV-PyMT transgenic mice, MMTV- Wnt-1 transgenic mice, MMTV/wild- type-neu transgenic mice, and MMTV- TGFα transgenic SD rat | High cost and time consuming | Intact immune function, genetic alterations are similar to human breast cancer patients, clear target, widely used for cancer studies, normal behaviors, and quick development of tumor |
| | Knockout | Tumor suppressor genes inactivation | Knockout mice of tumor susceptibility genes, such as p53, BRCA1/2, and pTEN. | | |

DMBA: 7,12-dimethylbenz(a) anthracene; NMU: n-methyl-nnitrosourea; SD: Sprague Dawley; NSG: NOD scid gamma mouse.

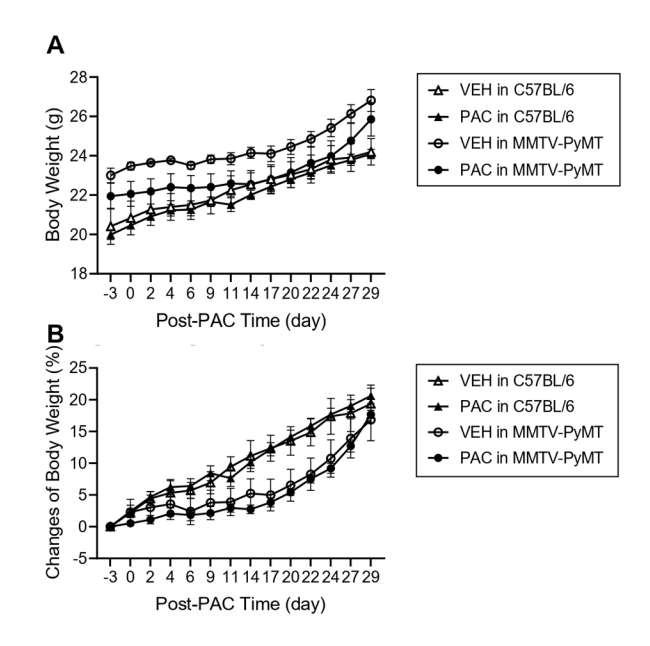


Figure 1. Changes of body weight in paclitaxel (PAC)- or vehicle (VEH)-injected C57BL/6 and tumor-bearing MMTV-PyMT mice. PAC (4 mg/kg) was injected intraperitoneally on four alternate days (days 0, 2, 4, and 6; cumulated doses of 16 mg/kg, downward arrows) in mice. VEH group received an equal volume (10 ml/kg) of 0.8% dimethyl sulfoxide and 0.8% Tween 80 in saline.

A. The mean of body weight of each group (n=8). **B**. The changes in body weight from the average weight at day 3. In the MMTV-PyMT mice, PAC (paclitaxel) was injected on day 0 when the breast tumor was about 0.5 cm. MMTV-PyMT mice showed a rapid increase in body weight after day 20. There was no significant difference in body weight between the groups of the same strain. Data are expressed as means \pm SEMs of 8 mice in each group.

paclitaxel, vehicle, or LGK-974. In each mouse, these reflexes were both scored as 0, meaning that paclitaxel, vehicle, and LGK-974 did not produce any sedation effects. Therefore, differences in positive responses in paclitaxel- and LGK-974—injected mice can be attributed to the treatments.

PINP model in C57BL/6 and breast tumorbearing MMTV-PyMT mice

Body weight of C57BL/6 and MMTV-PyMT mice injected with paclitaxel or vehicle was increased over 29 days after injections (Figure 1(a)). No significant differences in the changes of body weight were observed between Veh in C57BL/6 and PAC in C57BL/6 groups or between VEH in MMTV-PyMT or PAC in MMTV-PyMT groups (Figure 1(b)). It indicates that paclitaxel injections did not affect normal gain of body weight. When the 0.1-g von Frey filament was applied to the base of the third and fourth digits and the base of the fourth and fifth digits of the left hind paw (Figure 2(a)), normal mice exhibited a PPR ranging from 0% to 12% prior to paclitaxel injection. In the MMTV-PyMT mice, after paclitaxel injections on days 0, 2, 4, and 6, the PPR started to increase on day 4, peaked the highest levels (50%–60%) on

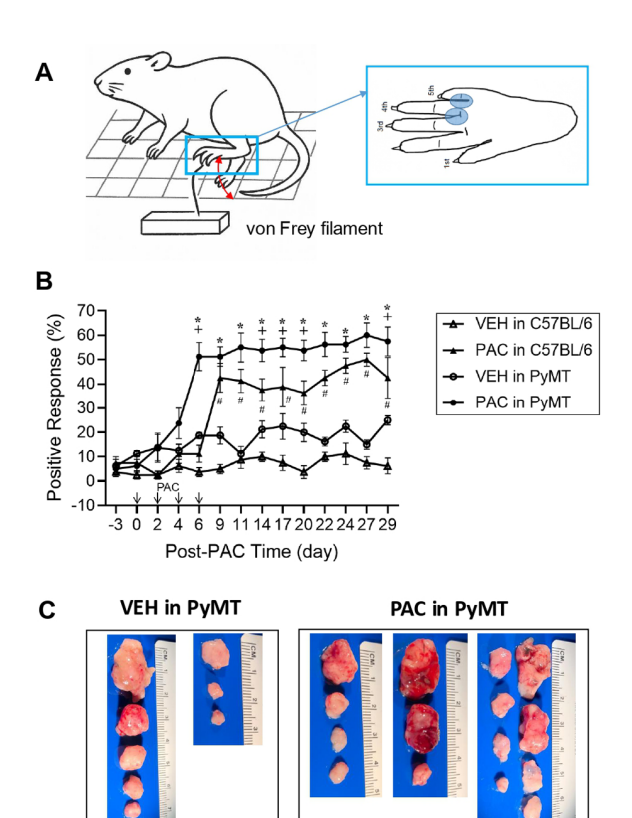


Figure 2. Development of neuropathic pain behaviors following paclitaxel administration in C57BL/6 and breast tumor-bearing MMTV-PyMT mice.

A. von Frey filament test and the site for von Frey filament application. B. The percentages of positive paw withdrawal responses to von Frey filament application in paclitaxel (PAC)- or vehicle (VEH)injected C57BL/6 and breast tumor-bearing MMTV-PyMT mice. PAC significantly increased the positive responses compared with the VEH groups in both C57BL/6 and MMTV-PyMT mice. In addition, PAC-injected MMTV-PyMT mice showed earlier induction of pain behavior compared to PAC-injected C57BL/6 mice. The vehicle groups did not exhibit pain behaviors. Data are expressed as means ± SEMs of 8 mice in each group. * and # indicate values in PAC-injected MMTV-PyMT and C57BL/6 mice significantly different (P<0.05) from corresponding values of VEH-injected MMTV-PyMT and VEH-injected C57BL/6 mice, respectively, based on using a two-way repeated measures analysis of variance with a repeated time factor, followed by Tukey multiple comparison test. + in PAC-injected MMTV-PyMT mice indicates values significantly different (P<0.05) from corresponding values of PAC-injected C57BL/6 mice. C. Breast tumor masses of representative MMTV-PyMT mice.

VEH-injected MMTV-PyMT mice (the left two mice) and PACinjected MMTV-PyMT mice (the three right mice) had various breast tumor masses on day 29.

days 6-9, and then plateaued for 29 days (n = 8). In the vehicle-injected MMTV-PyMT mice, the PPR increased to 20% after 29 days (n=8). In the paclitaxel-injected C57BL/6 mice, the PPR started to increase on day 6, peaked the highest levels (about 40%) on days 9-11, and then plateaued for 29 days

(n = 8). In the vehicle-injected C57BL/6 mice, the PPR did not significantly change (remaining less than 10%) for 29 days (n = 8). On days 6, 14, 17, 20, and 29, the PPR in paclitaxel-injected MMTV-PyMT mice significantly increased compared to that in C57BL/6 mice (Figure 2(b)). Compared to tumor-free mice, breast tumor-bearing mice exhibited an earlier onset and greater severity of paclitaxel-induced pain behaviors. To confirm whether tumors had formed properly in PyMT mice, vehicle and paclitaxel-injected PyMT mice were sacrificed on day 29 (last day) for tumor examination. All MMTV-PyMT mice including VEH in PyMT and PAC in PyMT groups had multiple breast tumors of varying sizes (Figure 2(c)).

Analgesic effects of single and multiple injections of a Wnt blocker LGK-97 4 on PINP in MMTV-PyMT mice

After pain behavior fully developed, on day 14 after the first paclitaxel injection, the MMTV-PyMT mice were intraperitoneally injected with varying doses of LGK-974 under blind conditions. A systemic administration of LGK-974 decreased the PPR in a dose-dependent manner at the 1, 3, and 10 mg/kg doses. In particular, LGK-974 at the 10 mg/kg decreased PPR by up to 20%, approaching the normal level before CIPN induction 1 hour and 1.5 hours after injection and returned to 60% 2.5 hours after injection (Figure 3(a)). In addition, the multiple injections of 10 mg/kg LGK-974 twice daily for 4 days on days 14–17 also significantly decreased the PPR on days 16-18 (Figure 3(b)). These data indicate that single and multiple injections of LGK-974 produce profound analgesic effects on PINP behaviors in breast tumor–bearing MMTV-PyMT mice.

Co-localization of β -catenin in mouse DRGs

Previous studies show that in adult mouse DRG, β-catening is present in neuronal nuclei and cytoplasm as well as in satellite glial cells, indicating diverse cellular localizations relevant to neuropathic pain.²¹ Building on these reports of neuronal and satellite-glial localization, the fluorescence intensity of β-catenin was measured in DRG neurons across three size categories ($\leq 30 \,\mu\text{m}$, $30-50 \,\mu\text{m}$, and $> 50 \,\mu\text{m}$) for each group (190 DRG neurons from C57BL/6-VEH (n = 4), 239 DRG neurons from MMTV-PyMT-VEH (n = 4) and 107 DRG neurons from MMTV-PyMT-PAC (n = 4) groups). In the C57BL/6-VEH group, the mean intensities of small $(\leq 30 \,\mu\text{m})$, medium $(30-50 \,\mu\text{m})$ and large $(>50 \,\mu\text{m})$ neurons were 24.96 ± 2.76 , 25.25 ± 4.12 , and 26.68 ± 3.60 , respectively. In the MMTV-PyMT-VEH group, corresponding values were 22.13 ± 2.27 , 23.15 ± 2.96 , and 25.35 ± 4.06 . For the MMTV-PyMT-PAC group, the values were $19.04 \pm$ 3.85, 17.89 ± 4.76 , and 19.80 ± 5.38 . Although a trend of

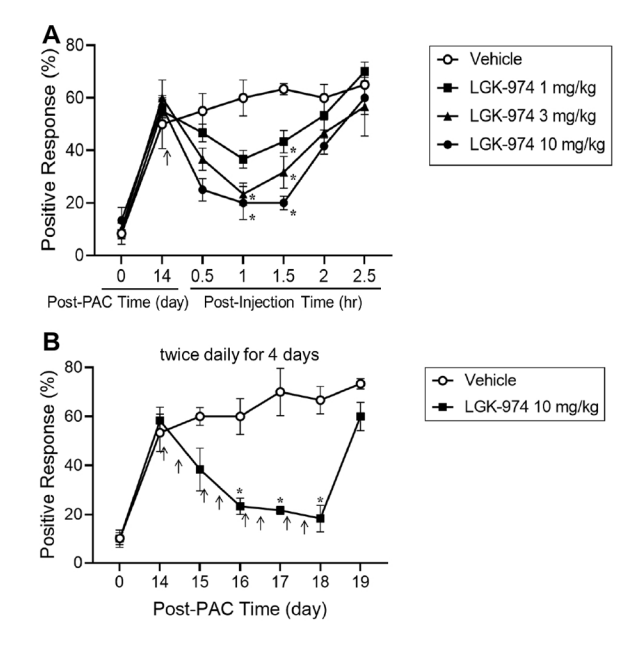


Figure 3. The analgesic effect of systemic single or multiple injections of LGK-974 on paclitaxel (PAC)-induced neuropathic pain in breast tumor—bearing MMTV-PyMT mice.

A. Effect of acute treatment of LGK-974 on paclitaxel-induced mechanical sensitivity in MMTV-PyMT mice.

On day 14 after the first injection of PAC, the 24 MMTV-PyMT mice were divided into four groups (n = 6 each): one that received the vehicle, and three that received various doses of LGK-974. The single $10\,\text{mg/kg}$ dose of LGK-974 significantly decreased the positive response 1 and 1.5 hours after injection in a dose-dependent manner. Data are expressed as means \pm SEMs.

B. Effect of repeated administration of LGK-974 on paclitaxel-induced mechanical sensitivity in MMTV-PyMT mice. On day 14, the 12 PAC-injected MMTV-PyMT mice were divided into two groups (n = 6 each): one that received the vehicle and one that received $10\,\text{mg/kg}$ LGK-974 at 12-h intervals twice daily for 4 days starting at day 14. Positive responses were measured once a day before injection of LGK-974. Multiple injections of LGK-974 significantly decreased the positive responses on day 16 and maintained the decreased response for 3 days. Data are expressed as means \pm SEMs. Asterisks indicate significant differences from the vehicle group based on a two-way repeated-measures analysis of variance with a repeated time factor, followed by Tukey multiple comparison test.

increasing intensity with cell size was observed in the C57BL/6-VEH and MMTV-PyMT-VEH groups, and a non-monotonic pattern in the MMTV-PyMT-PAC group, statistical analysis revealed no significant differences across size categories among each group (p > 0.05, data not shown). Active β -catenin was expressed in the L4 and L5 DRGs of vehicle- and paclitaxel-injected C57BL/6 and MMTV-PyMT mice. Expression of β -catenin was localized with the NeuN-expressing neurons (Figure 4(a)). Further, the expression of β -catenin was localized with CGRP-expressing neurons (Figure 4(b)) and GFAP-expressing satellite cells (Figure 4(c)). These data indicate that active β -catenin was co-localized in mouse DRG neurons, including CGRP-expressing cells, and satellite cells.

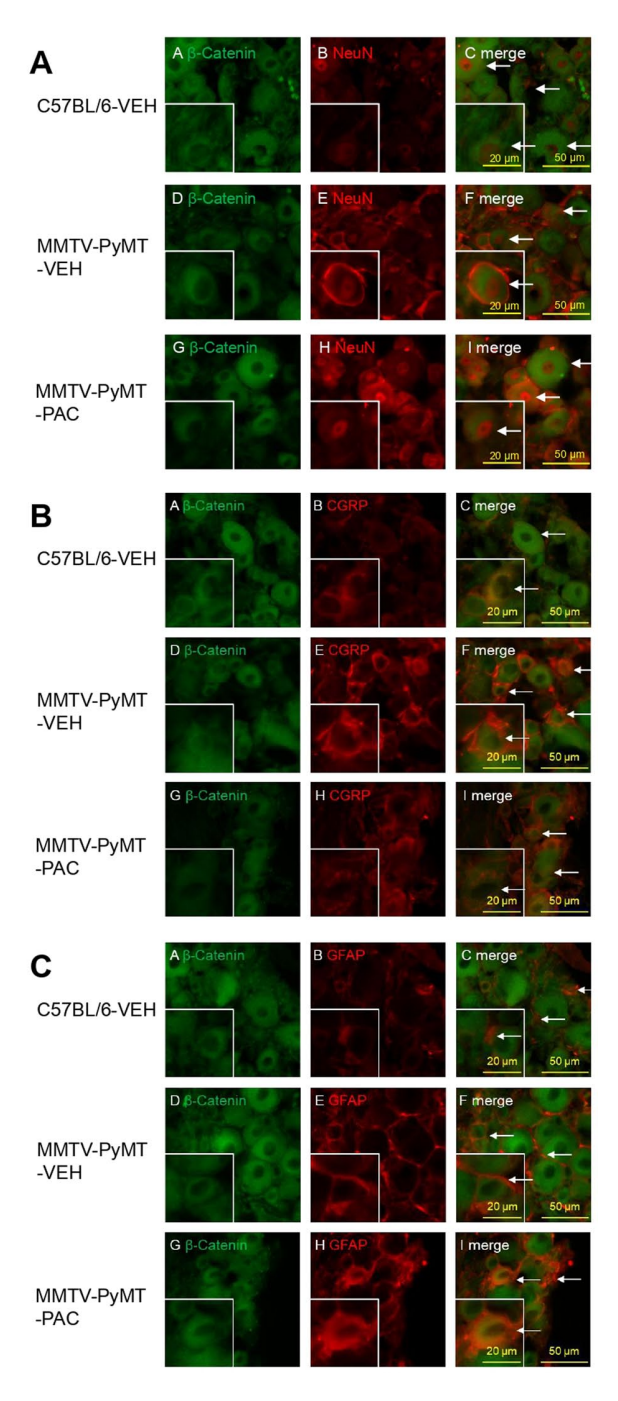


Figure 4. Expression of β -catenin, a canonical Wnt signaling marker, in neurons in dorsal root ganglia (DRGs) of C57BL/6 and tumor-bearing MMTV-PyMT mice.

A. Co-localization of β -catenin in the neurons of mouse L4 and L5 DRGs. (A) active β -catenin, (B) mouse neuron marker (NeuN), and (C) β -catenin and NeuN in the DRGs from the VEH-injected C57BL/6. Arrow indicates β -catenin with NeuN. (D) β -catenin, (E) NeuN, and (F) β -catenin and NeuN in the DRGs from the VEH-injected MMTV-PyMT. Arrow indicates β -catenin with NeuN in DRG. (G) β -catenin, (H) NeuN, and (I) β -catenin and NeuN in the DRG from the PAC-injected MMTV-PyMT. β -catenin was expressed with NeuN in the DRGs from the PAC-injected MMTV-PyMT. Arrow indicates β -catenin with NeuN. Scale bars were 20 μ m in the inset and 50 μ m in the main images. Green, β -catenin; red, NeuN.

B. Co-localization of β -catenin in calcitonin gene-related peptide (CGRP)–expressing neurons in mouse DRGs. (A) β -catenin, (B) CGRP, and (C) β -catenin (green) and CGRP (red) in the DRGs from the VEH-injected C57BL/6. Arrow indicates β -catenin with CGRP-expressing neuron. (D) β -catenin, (E) CGRP, and (F) β -catenin and CGRP in the DRGs from the VEH-injected MMTV-PyMT. Arrow indicates β -catenin with CCRP-expressing neuron. (G) β -catenin, (H) CGRP, and (I) β -catenin (green) and CGRP (red) in the DRG from the PAC-injected MMTV-PyMT. Arrow indicates where β -catenin was expressed with CGRP-expressing neurons. Scale bars were 20 μm in the inset and 50 μm in the main images. Green, β -catenin; red, CGRP. **C.** Co-localization of β -catenin in glial fibrillary acidic protein (GFAP)-expressing satellite cells in mouse DRGs. (A) β -catenin, (B) GFAP, and (C) β -catenin

C. Co-localization of β-catenin in glial fibrillary acidic protein (GFAP)-expressing satellite cells in mouse DRGs. (A) β-catenin, (B) GFAP, and (C) β-catenin and GFAP in the DRGs from the VEH-injected C57BL/6. Arrow indicates β-catenin with GFAP-expressing satellite cells. (D) β-Catenin, (E) GFAP, and (F) β-catenin and GFAP in the DRGs from the VEH-injected MMTV-PyMT. Arrow indicates β-catenin with GFAP-expressing satellite cells. (G) β-catenin, (H) GFAP, and (I) β-catenin and GFAP in the DRGs from the PAC-injected MMTV-PyMT. Arrow indicates where β-catenin was expressed with GFAP-expressing satellite cells in the DRGs. Scale bars were 20 μm in the inset and 50 μm in the main image.

Discussion

The present study showed that tumor–bearing mice exhibited an earlier onset and greater severity of paclitaxel-induced pain behaviors than naive mice. Single or multiple injections of LGK-974, a Wnt/ β -catenin blocker, alleviated pain behaviors. The activation of β -catenin was detected in neurons including CGRP-expressing neurons and satellite cells in the DRG of MMTV-PyMT mice. These results suggest that the tumor-bearing animal model may better replicate the clinical conditions of CIPN in human and targeting Wnt/ β -catenin signaling may offer a novel approach in managing neuropathic pain, particularly in breast-tumor patients who experience CIPN.

As reported in previous publications, 22-25 MMTV-PyMT mice showed rapid development of multifocal tumors. It was reported that MMTV-PyMT mice develop hyperplasia at 4-6 weeks, mammary intraepithelial neoplasia at 7-9 weeks, early carcinoma at 8-12 weeks, and late carcinoma at 10-14 weeks.²² End-stage tumors infiltrate various immune cells, including macrophage and T lymphocytes.²⁶ In the tumor microenvironment in MMTV-PyMT mice, the amount of mammary tissue macrophages decrease, and the amount of tumor-associated macrophages increase.^{27,28} Macrophages can promote cancer metastasis, including tumor invasion, cell extravasation, and colonization.²⁸ During prognosis, macrophages are polarized to M1 macrophages that produce proinflammatory cytokines and antigen presentation.^{28,29} In addition, the number of CD4+ T lymphocytes increase during tumor progression.³⁰ When CD4+ T lymphocytes were depleted, circulating tumor cells and pulmonary metastasis were reduced.³⁰ Also an influx of neutrophils occurs in the pre-metastatic lung of MMTV-PyMT mice.³¹ In comparison, natural killer cells reduced pulmonary metastasis.³² In sum, MMTV-PyMT mice produce spontaneous breast tumors and have intact immune functions. Taken together, MMTV-PyMT mice have rapid developed breast tumors with immune cells.

Breast cancer is classified by gene expression into five subtypes including 1) luminal, 2) epidermal growth factor receptor 2 (HER2)-amplified, 3) basal, 4) normal breastlike, and 5) Claudin-low. 10,33 Luminal breast cancers are generally positive for estrogen receptor (ER) and negative for HER2 amplification and divided into two subtypes: luminal A and luminal B. 19,34 Luminal A (ER+PR+HER2-) is less sensitive to chemotherapy.¹⁹ However, luminal B (ER+PR+HER2+) is more sensitive to chemotherapy.¹⁹ HER2-amplified tumors (ER-PR-HER2+) harbor amplification of the HER2 gene and display overexpression of other genes close to HER2.¹⁹ Basal breast cancers (ER-PR-HER2-), also called triple-negative breast cancer, are ER/ progesterone receptor (PR)-negative and HER2-negative tumors and show chemoresistance. 19,35 Typical breast-like tumors have a gene expression profile of nonmalignant normal breast epithelium.³⁶ Lastly, claudin-low cancers show strong triple-negative expression of ER, PR, and HER2 with

low expression of cell-cell junction proteins, including E-cadherin.³⁷ The prognosis of patients with these breast cancer types ranges, with those with luminal A having the best prognosis, followed by those with luminal B, HER2 overexpression, and basal. In this study, we used MMTV-PyMT mice. Their gene expression profiling shows the luminal B subtype of human breast cancer and displayed loss of ER/Esr1 and PR/Pgr and overexpression of ErbB2 and cyclin D1/Ccnd1.^{25,38,39} Therefore, our new CINP model belongs among the luminal B breast cancer models.

Paclitaxel and docetaxel are mainly used to treat earlystage and metastatic breast cancer. They produce peripheral neuropathy in 30% to 97% of breast cancer patients, and 47% of these patients have neuropathy 6 years after chemotherapy.³ In this study, we used paclitaxel as chemotherapy. Many chemotherapeutic drugs, including alkylating agents (cyclophosphamide), anthracyclines (doxorubicin and epirubicin), and antimetabolites (5-fluorouracil, capecitabine, and methotrexate), are widely used for breast cancer patients and produce neuropathy.40 The present study showed that breast tumor-bearing mice began to exhibit increased pain behaviors approximately 2 to 4 days following paclitaxel treatments, compared to tumor-free mice. It was reported that initial symptoms of paclitaxel-induced peripheral neuropathy typically emerge within 1-3 days in the patients with cancer. 41 It suggests that the tumor-bearing animal model may better replicate the clinical conditions of CIPN in human. In addition, these results suggest that tumor-derived factors may significantly contribute to the development and exacerbation of neuropathic pain, particularly in breast cancer patients undergoing paclitaxel chemotherapy. Identifying these factors may be crucial for understanding the mechanisms underlying CIPN and for developing targeted interventions. 41,42

In this study, LGK-974 produced analgesic effects on the PINP in MMTV-PyMT mice. LGK-974 is an inhibitor of Wnt ligand secretion in the Wnt/β-catenin signaling pathway (the canonical Wnt pathway). 43,44 The Wnt pathway has roles in cell proliferation, cancer development, synapse maturation, neuronal plasticity, and the regulation of N-methyl-D-aspartate receptors. 45,46 In the presence of Wnt ligands, the binding of Wnt ligands to cell surface receptors composed of the Frizzled receptor and LRP5/6 co-receptor, activates the Dishevelled protein, 47 inhibiting the protein destruction complex of adenomatous polyposis coli, glycogen synthase kinase 3, and Axin proteins. 48 As a result, the stabilized β-catenin, a key mediator of Wnt signaling, moves into the nucleus and activates Wnt target genes. 48 The deregulation of Wnt/β-catenin signaling is involved in cancer.⁴⁸ LGK-974 has been reported to show anti-cancer effects on Wnt signaling-associated human cancers (i.e. melanoma, basal breast cancer, head and neck cancer, pancreatic cancer, cervical cancer, and lung cancer) in preclinical and clinical studies. 44,49-51 In addition, several Wnt blockers produced analgesic effects on various neuropathic pain models. 15,16,52 Hence, LGK-974 may produce both analgesia and

anti-cancer effects in CINP in cancer patients, which means when a treatment protocol combines LGK-974 and paclitaxel, LGK-974 may decrease the dose of paclitaxel and then decrease CINP.

In this study, we reported that active β -catenin was expressed in neurons including CGRP-expressing neurons and satellite cells in the DRG of MMTV-PyMT mice. In the DRG neurons, CGRP-expressing neurons are mostly C fibers with some $A\beta$ and $A\delta$ fibers, which means active β -catenin was expressed in C, $A\beta$, and $A\delta$ fibers in MMTV-PyMT mice. Satellite cells in MMTV-PyMT mice. Our data suggest that the Wnt/ β -catenin pathway may be expressed in the sensory nerve tissues.

This study has clear limitations. First, we used only paclitaxel as the CINP-inducing chemotherapy. Second, we used only LGK-974 as a reference drug. Future studies should include other CINP-inducing drugs and other medicines such as gabapentin.

Conclusions

In conclusion, paclitaxel can produce neuropathic pain in breast tumor–bearing MMTV-PyMT mice, resulting in a much-needed CINP model in breast tumor–bearing mice. LGK-974, a Wnt/ β -catenin signaling blocker, shows analgesic effects in breast tumor–bearing mice with CINP, potential antitumor effects were not assessed here and warrant dedicated study. Additionally, active β -catenin was colocalized with neurons, CGRP-expressing neurons, and satellite cells in breast tumor–bearing mice. Therefore, the PINP model in breast tumor–bearing MMTV-PyMT mice may be beneficial for studying: 1) the analgesic effects and mechanisms for CINP; 2) both CINP and cancer.

List of Abbreviations

Abbreviation Full Term

CIPN Chemotherapy-Induced Peripheral Neuropathy
CINP Chemotherapy-Induced Neuropathic Pain

DRG Dorsal Root Ganglion

CGRP Calcitonin Gene-Related Peptide GFAP Glial Fibrillary Acidic Protein

LGK-974 Porcupine Inhibitor LGK-974 (Wnt/β-catenin

pathway inhibitor)

MMTV-PyMT Mouse Mammary Tumor Virus-Polyomavirus

Middle T Antigen

PAC Paclitaxel

PINP Paclitaxel-Induced Neuropathic Pain PPR Percentage of Positive Paw Withdrawal

> Responses Vehicle

VEH Vehicle

ER Estrogen Receptor
PR Progesterone Receptor

HER2 Human Epidermal Growth Factor Receptor 2
What Wingless related integration site (cigneling

Wnt Wingless-related integration site (signaling

pathway)

DMSO Dimethyl Sulfoxide

SEM Standard Error of the Mean

LRP5/6 Low-Density Lipoprotein Receptor-Related

Protein 5/6

Acknowledgments

The authors thank Ashli Nguyen-Villarreal and Sarah Bronson (Editing Services, Research Medical Library, The University of Texas MD Anderson Cancer Center) for their editorial assistance with this manuscript.

Authors contributions

HK designed and performed the experiments, analyzed data, and drafted the manuscript. YSJ and JP contributed to data interpretation. JX, JK and SA participated in data collection. HYK, JX and HK supervised the study and contributed to manuscript revision. All authors read and approved the final manuscript. Hee Kee Kim and Juping Xing contributed equally to this work and share first authorship.

Declaration of Conflicting Interests

The authors declared no potential conflicts of interest with respect to the research, authorship, and/or publication of this article.

Funding

The authors disclosed receipt of the following financial support for the research, authorship, and/or publication of this article: This work was supported by the Cancer Prevention Research Institute of Texas (RP200314 to JP), the National Cancer Institute (CA193297 to JP), grants from the Peggy and Avinash Ahuja Foundation and the Helen Buchanan and Stanley Joseph Seeger Endowment at The University of Texas MD Anderson Cancer Center (to SA), and a faculty research grant of Yonsei University College of Medicine (6-2022-0182 and 6-2023-0214), the National Research Foundation of Korea(NRF) grant founfed by the Korea government(MSIT) RS-2025-00555096, Korea Institute of Oriental Medicine Grants KSN2511011 (to HYK).

Ethics approval and consent to participate.

All animal procedures were approved by the Institutional Animal Care and Use Committee (IACUC) at The University of Texas MD Anderson Cancer Center (No.00001569-RN00 and 11-12-12541). All experiments were conducted in accordance with relevant ARRIVE guidelines and regulations.

Consent for publication

Not applicable.

ORCID iDs

Juping Xing https://orcid.org/0009-0001-3259-4347 Hee Young Kim https://orcid.org/0000-0002-2495-9115

Availability of data and materials

The datasets generated and/or analyzed during the current study are available from the corresponding author on reasonable request.

References

- Chung M, Kim HK, Abdi S. Update on cannabis and cannabinoids for cancer pain. Curr Opin Anaesthesiol 2020; 33(6): 825–831
- Hou S, Huh B, Kim HK, Kim KH, Abdi S. Treatment of chemotherapy-induced peripheral neuropathy: systematic review and recommendations. *Pain Physician* 2018; 21(6): 571–592.
- Massey RL, Kim HK, Abdi S. Brief review: chemotherapyinduced painful peripheral neuropathy (CIPPN): current status and future directions. Can J Anaesth 2014; 61(8): 754–762.
- Sharifi-Rad J, Quispe C, Patra JK, Singh YD, Panda MK, Das G, Adetunji CO, Rapposelli S, Nagle V, Herrera-Bravo J, Kaushik D, Suleria HAR, Salazar LA, Docea AO, Calina D. Paclitaxel: application in modern oncology and nanomedicine-based cancer therapy. *Oxid Med Cell Longev* 2021; 2021: 3687700.
- Kankowski S, Grothe C, Haastert-Talini K. Neuropathic pain: spotlighting anatomy, experimental models, mechanisms, and therapeutic aspects. *Eur J Neurosci* 2021; 54(2): 4475–4496.
- Saraiva-Santos T, Zaninelli TH, Pinho-Ribeiro FA. Modulation of host immunity by sensory neurons. *Trends Immunol* 2024; 45(5): 381–396.
- Huang S, Zhu J, Yu L, Huang Y, Hu Y. Cancer-nervous system crosstalk: from biological mechanism to therapeutic opportunities. *Mol Cancer* 2025; 24(1): 133.
- Tanaka K, Kondo T, Narita M, Muta T, Yoshida S, Sato D, Suda Y, Hamada Y, Shimizu T, Kuzumaki N, Narita M. Cancer aggravation due to persistent pain signals with the increased expression of pain-related mediators in sensory neurons of tumor-bearing mice. *Mol Brain* 2023; 16(1): 19.
- Green VL. Breast cancer risk assessment and management of the high-risk patient. Obstet Gynecol Clin North Am 2022; 49(1): 87–116.
- Zeng L, Li W, Chen CS. Breast cancer animal models and applications. Zool Res 2020; 41(5): 477–494.
- 11. Gross ETE, Han S, Vemu P, Peinado CD, Marsala M, Ellies LG, Bui JD. Immunosurveillance and immunoediting in MMTV-PyMT-induced mammary oncogenesis. *Oncoimmunology* 2017; 6(2):e1268310.
- Attalla S, Taifour T, Bui T, Muller W. Insights from transgenic mouse models of PyMT-induced breast cancer: recapitulating human breast cancer progression in vivo. *Oncogene* 2021; 40(3): 475–491.
- King TD, Suto MJ, Li Y. The Wnt/β-catenin signaling pathway: a potential therapeutic target in the treatment of triple negative breast cancer. *J Cell Biochem* 2012; 113(1): 13–18.
- 14. Gangrade A, Pathak V, Augelli-Szafran CE, Wei H-X, Oliver P, Suto M, Buchsbaum DJ. Preferential inhibition of Wnt/β-catenin signaling by novel benzimidazole compounds in triple-negative breast cancer. *Int J Mol Sci* 2018; 19(5): 1524.
- Tang J, Ji Q, Jin L, Tian M, Zhang LD, Liu XY. Secreted frizzled-related protein 1 regulates the progression of neuropathic pain in mice following spinal nerve ligation. *J Cell Physiol* 2018; 233(8): 5815–5822.
- Kim HK, Bae J, Lee SH, Hwang SH, Kim MS, Kim MJ, Lee JH, Cho H, Park JS, Choi YH. Blockers of Wnt3a, Wnt10a, or beta-Catenin Prevent Chemotherapy-Induced Neuropathic Pain In Vivo. *Neurotherapeutics* 2021; 18(1): 601–614.

17. Kim E, Hwang SH, Kim HK, Abdi S, Kim HK. Losartan, an Angiotensin II Type 1 Receptor Antagonist, Alleviates Mechanical Hyperalgesia in a Rat Model of Chemotherapy-Induced Neuropathic Pain by Inhibiting Inflammatory Cytokines in the Dorsal Root Ganglia. *Mol Neurobiol* 2019; 56(11): 7408–7419.

- Kim HK, Zhang YP, Gwak YS, Abdi S. Phenyl N-tertbutylnitrone, a free radical scavenger, reduces mechanical allodynia in chemotherapy-induced neuropathic pain in rats. *Anesthesiology* 2010; 112(2): 432–439.
- Holen I, Speirs V, Morrissey B, Blyth K. In vivo models in breast cancer research: progress, challenges and future directions. *Dis Model Mech* 2017; 10(4): 359–371.
- Ionkina AA, Balderrama-Gutierrez G, Ibanez KJ, Phan SHD, Cortez AN, Mortazavi A, Chen EY, Nguyen T, Smith RE, Johnson RM. Transcriptome analysis of heterogeneity in mouse model of metastatic breast cancer. *Breast Cancer Res* 2021; 23(1): 93.
- Duraikannu A, Martinez JA, Chandrasekhar A, Zochodne DW. Expression and Manipulation of the APC-β-Catenin Pathway During Peripheral Neuron Regeneration. *Scientific Reports* 2018; 8(1): 13197.
- Varticovski L, Hollingshead MG, Robles AI, Wu X, Cherry J, Munroe DJ, Wang W, Mirkovic N, Jenkins RB, Hayes DN. Accelerated preclinical testing using transplanted tumors from genetically engineered mouse breast cancer models. *Clin Cancer Res* 2007; 13(7): 2168–2177.
- 23. Almholt K, Juncker-Jensen A, Laerum OD, Dano K, Johnsen M, Lund LR, Rygaard J, Romer J, Nielsen BS, Lademann U. Metastasis is strongly reduced by the matrix metalloproteinase inhibitor Galardin in the MMTV-PymT transgenic breast cancer model. *Mol Cancer Ther* 2008; 7(9): 2758–2767.
- Almholt K, Lund LR, Rygaard J, Nielsen BS, Dano K, Romer J, Lademann U, Laerum OD, Johnsen M. Reduced metastasis of transgenic mammary cancer in urokinase-deficient mice. *Int J Cancer* 2005; 113(4): 525–532.
- Lin EY, Jones JG, Li P, Zhu L, Whitney KD, Muller WJ, Pollard JW. Progression to malignancy in the polyoma middle T oncoprotein mouse breast cancer model provides a reliable model for human diseases. *Am J Pathol* 2003; 163(5): 2113– 2126.
- Ekiz HA, Lai SA, Gundlapalli H, Haroun F, Williams MA, Welm AL. Inhibition of RON kinase potentiates anti-CTLA-4 immunotherapy to shrink breast tumors and prevent metastatic outgrowth. *Oncoimmunology* 2018; 7(9):e1480286.
- Franklin RA, Liao W, Sarkar A, Kim MV, Bivona MR, Liu K, Pamer EG, Li MO, Rudensky AY, Li B. The cellular and molecular origin of tumor-associated macrophages. *Science* 2014; 344(6186): 921–925.
- Lin Y, Xu J, Lan H. Tumor-associated macrophages in tumor metastasis: biological roles and clinical therapeutic applications. *J Hematol Oncol* 2019; 12(1): 76.
- 29. Ostuni R, Kratochvill F, Murray PJ, Natoli G. Macrophages and cancer: from mechanisms to therapeutic implications. *Trends Immunol* 2015; 36(4): 229–239.
- DeNardo DG, Barreto JB, Andreu P, Vasquez L, Tawfik D, Kolhatkar N, Coussens LM. CD4(+) T cells regulate pulmonary metastasis of mammary carcinomas by enhancing

- protumor properties of macrophages. *Cancer Cell* 2009; 16(2): 91–102.
- Wculek SK, Malanchi I. Neutrophils support lung colonization of metastasis-initiating breast cancer cells. *Nature* 2015; 528(7582): 413–417.
- Ohs I, Ducimetiere L, Marinho J, Kulig P, Becher B, Tugues S. Restoration of Natural Killer Cell Antimetastatic Activity by IL12 and Checkpoint Blockade. *Cancer Res* 2017; 77(24): 7059–7071.
- 33. Cardiff RD, Kenney N. A compendium of the mouse mammary tumor biologist: from the initial observations in the house mouse to the development of genetically engineered mice. *Cold Spring Harb Perspect Biol* 2011; 3(6).
- 34. Yanagawa M, Ikemot K, Kawauchi S, Furuya T, Yamamoto S, Oka M, Komatsu Y, Horiguchi J, Tanaka N. Luminal A and luminal B (HER2 negative) subtypes of breast cancer consist of a mixture of tumors with different genotype. *BMC Res Notes* 2012; 5: 376.
- 35. Seal MD, Chia SK. What is the difference between triple-negative and basal breast cancers? *Cancer J* 2010; 16(1): 12–16.
- Sørlie T, Perou CM, Tibshirani R, Aas T, Geisler S, Johnsen H, Hastie T, Eisen MB, van de Rijn M, Jeffrey SS. Gene expression patterns of breast carcinomas distinguish tumor subclasses with clinical implications. *Proc Natl Acad Sci U S A* 2001; 98(19): 10869–10874.
- Sabatier R, Finetti P, Guille A, Adelaide J, Chaffanet M, Viens P, Birnbaum D. Claudin-low breast cancers: clinical, pathological, molecular and prognostic characterization. *Mol Cancer* 2014; 13: 228.
- Maglione JE, Moghanaki D, Young LJ, Manner CK, Ellies LG, Joseph SO, Cardiff RD. Transgenic Polyoma middle-T mice model premalignant mammary disease. *Cancer Res* 2001; 61(22): 8298–8305.
- 39. Owyong M, Chou J, van den Bijgaart RJ, Kong N, Efe G, Maynard C, Hartley R, Zheng X. MMP9 modulates the metastatic cascade and immune landscape for breast cancer antimetastatic therapy. *Life Sci Alliance* 2019; 2(6).
- 40. von Minckwitz G, Conrad B, Reimer T, Decker T, Eidtmann H, Eiermann W, Gerber B, Kummel S, Lauer T, Thomssen C. A randomized phase 2 study comparing EC or CMF versus nab-paclitaxel plus capecitabine as adjuvant chemotherapy for nonfrail elderly patients with moderate to high-risk early breast cancer (ICE II-GBG 52). Cancer 2015; 121(20): 3639–3948.
- 41. Argyriou AA, Koltzenburg M, Polychronopoulos P, Papapetropoulos S, Kalofonos HP. Peripheral nerve damage

- associated with administration of taxanes in patients with cancer. *Crit Rev Oncol Hematol* 2008; 66(3): 218–228.
- 42. Dougherty PM, Cata JP, Cordella JV, Burton A, Weng HR. Taxol-induced sensory disturbance is characterized by preferential impairment of myelinated fiber function in cancer patients. *Pain* 2004; 109(1): 132–142.
- 43. Kina S, Kawabata-Iwakawa R, Miyamoto S, Arasaki A, Sunakawa H, Kinjo T, Sakamoto M, Takeda M. A molecular signature of well-differentiated oral squamous cell carcinoma reveals a resistance mechanism to metronomic chemotherapy and novel therapeutic candidates. *J Drug Target* 2021; 29(10): 1118–1127.
- 44. Tang Y, Jiang M, Chen A, Qu W, Han X, Zuo J, Wang Z, Li X, Liu C. Porcupine inhibitor LGK974 inhibits Wnt/betacatenin signaling and modifies tumorassociated macrophages resulting in inhibition of the malignant behaviors of nonsmall cell lung cancer cells. *Mol Med Rep* 2021; 24(2).
- Nusse R, Clevers H. Wnt/beta-Catenin Signaling, Disease, and Emerging Therapeutic Modalities. *Cell* 2017; 169(6): 985–99.
- Oliva CA, Montecinos-Oliva C, Inestrosa NC. Wnt Signaling in the Central Nervous System: New Insights in Health and Disease. *Prog Mol Biol Transl Sci* 2018; 153: 81–130.
- Rosso SB, Sussman D, Wynshaw-Boris A, Salinas PC. Wnt signaling through Dishevelled, Rac and JNK regulates dendritic development. *Nat Neurosci* 2005; 8(1): 34–42.
- 48. Clevers H, Nusse R. Wnt/beta-catenin signaling and disease. *Cell* 2012; 149(6): 1192–1205.
- Jung YS, Park JI. Wnt signaling in cancer: therapeutic targeting of Wnt signaling beyond beta-catenin and the destruction complex. *Exp Mol Med* 2020; 52(2): 183–191.
- Bao J, Lee HJ, Zheng JJ. Genome-wide network analysis of Wnt signaling in three pediatric cancers. *Sci Rep* 2013; 3: 2969.
- 51. Shah K, Panchal S, Patel B. Porcupine inhibitors: Novel and emerging anti-cancer therapeutics targeting the Wnt signaling pathway. *Pharmacol Res* 2021; 167: 105532.
- Xu Z, Chen Y, Yu J, Yin D, Liu C, Chen X, Wang J, Li H. TCF4 Mediates the Maintenance of Neuropathic Pain Through Wnt/beta-Catenin Signaling Following Peripheral Nerve Injury in Rats. *J Mol Neurosci* 2015; 56(2): 397–408.
- Ishida-Yamamoto A, Senba E, Tohyama M. Calcitonin generelated peptide- and substance P-immunoreactive nerve fibers in Meissner's corpuscles of rats: an immunohistochemical analysis. *Brain Res* 1988; 453(1–2): 362–366.